

Year: 2010

## **Recapitulation of endochondral bone formation using human adult mesenchymal stem cells as a paradigm for developmental engineering**

Scotti, Celeste and Tonnarelli, Beatrice and Papadimitropoulos, Adam and Scherberich, Arnaud and Schaeren, Stefan and Schauerte, Alexandra and Lopez-Rios, Javier and Zeller, Rolf and Barbero, Andrea and Martin, Ivan

Posted at edoc, University of Basel

Official URL: <http://edoc.unibas.ch/dok/A6003625>

Originally published as:

Scotti, Celeste and Tonnarelli, Beatrice and Papadimitropoulos, Adam and Scherberich, Arnaud and Schaeren, Stefan and Schauerte, Alexandra and Lopez-Rios, Javier and Zeller, Rolf and Barbero, Andrea and Martin, Ivan. (2010) *Recapitulation of endochondral bone formation using human adult mesenchymal stem cells as a paradigm for developmental engineering*. Proceedings of the National Academy of Sciences of the United States of America, Vol. 107, H. 16. S. 7251-7256.

**RECAPITULATION OF ENDOCHONDRAL BONE FORMATION  
USING HUMAN ADULT MESENCHYMAL STEM CELLS: A  
PARADIGM FOR DEVELOPMENTAL ENGINEERING**

<sup>1,2\*</sup>Celeste Scotti, <sup>1\*</sup>Beatrice Tonnarelli, <sup>1</sup>Adam Papadimitropoulos, <sup>1</sup>Arnaud Scherberich,  
<sup>1</sup>Stefan Schaeren, <sup>3</sup>Alexandra Schauerte, <sup>3</sup>Javier Lopez-Rios, <sup>3</sup>Rolf Zeller, <sup>1#</sup>Andrea Barbero,  
<sup>1#</sup>Ivan Martin

<sup>1</sup>Departments of Surgery and of Biomedicine, University Hospital Basel, Hebelstrasse 20,  
4056, Basel, Switzerland

<sup>2</sup>Residency Program in Orthopaedics and Traumatology, Università degli Studi di Milano,  
Milano, Italy

<sup>3</sup>Developmental Genetics, Department of Biomedicine, University of Basel, Mattenstrasse 28,  
4058, Basel, Switzerland

\*C.S. and B.T. contributed equally to this study

#Corresponding authors

**Address correspondence to:** Ivan Martin and Andrea Barbero

ICFS, University Hospital Basel

Hebelstrasse 20, ZLF, Room 405

4031 Basel, Switzerland

Phone: + 41 61 265 2384; fax: + 41 61 265 3990

e-mail: [imartin@uhbs.ch](mailto:imartin@uhbs.ch); [abarbero@uhbs.ch](mailto:abarbero@uhbs.ch)

**Manuscript information:** 19 pages, 5 figures

## **ABSTRACT**

Mesenchymal Stem/Stromal Cells (MSC) are typically used to generate bone tissue by a process resembling intra-membranous ossification, i.e. by direct osteoblastic differentiation. However, most bones develop by endochondral ossification, i.e. via remodeling of hypertrophic cartilaginous templates. To date, endochondral bone formation has not been successfully reproduced using human, clinically compliant cell sources. Here, we aimed at engineering tissues from bone marrow-derived, adult human MSC with an intrinsic capacity to undergo endochondral ossification. By analogy to embryonic limb development, we hypothesized that successful execution of the endochondral ossification program depends on the initial formation of hypertrophic cartilaginous templates. Human MSC, subcutaneously implanted into nude mice at various stages of chondrogenic differentiation, formed interconnected bone trabeculae only when they had developed *in vitro* hypertrophic tissue structures. Advanced maturation *in vitro* resulted in accelerated formation of larger bony tissues. The underlying morphogenetic process was structurally and molecularly similar to the temporal and spatial progression of limb bone development in embryos. In particular, Indian Hedgehog signalling was activated at early stages and required for the *in vitro* formation of hypertrophic cartilage. Subsequent development of a bony collar *in vivo* was followed by vascularisation, osteoclastic resorption of the cartilage template and appearance of hematopoietic foci. This study reveals the capacity of human MSC to generate bone tissue via an endochondral ossification program and provides a valid model to study mechanisms governing bone development. Most importantly, this process could be engineered to generate advanced grafts for bone regeneration by invoking a “developmental engineering” paradigm.

## **KEYWORDS**

endochondral ossification; hypertrophic chondrocytes; bone development; regenerative medicine; tissue engineering

\body

## **INTRODUCTION**

Endochondral ossification, namely the formation of bone tissue by replacement of cartilage templates, is the route through which long bones and the axial skeleton are formed in developing embryos (1). This process relies on the highly specialized morpho-regulatory functions of hypertrophic chondrocytes (2). Hypertrophic chondrocytes derive from the initial condensation of mesenchymal precursors and begin to produce a type X collagen-rich avascular cartilaginous matrix. At the periphery of this cartilage tissue, the so called “borderline” hypertrophic chondrocytes (3) instruct surrounding mesenchymal cells to differentiate into osteoblasts, which results in formation of the typical “bony collar”. In parallel, chondrocytes in the central regions direct mineralization of the hypertrophic cartilage by initiating remodeling via the production of specific matrix metalloproteinases (MMP) and attract blood vessels by releasing vascular-endothelial growth factor (VEGF). The in-growing blood vessels deliver osteoblastic, osteoclastic and hematopoietic precursors, which mediate resorption of the deposited cartilaginous template and formation of vascularized bone tissue containing the so-called stromal sinusoids, which provide the microenvironment for hematopoiesis (1).

Mesenchymal stem/stromal cells (MSC) from human adults have the ability to generate bone tissue in a variety of experimental models (4), and hold great potential for bone repair in regenerative medicine. Thus far, MSC have been shown to generate bone tissue exclusively through direct osteogenic differentiation (i.e. in a manner akin to intra-membranous ossification), using a mineralized surface as “priming” substrate, with the exception of implantation in confined environments that prevent blood vessel invasion (e.g. diffusion chambers; ref. 5, 6). This approach has already been used for a few clinical trials (7), but has not been effective for wide-spread clinical application (4). The possibility to engineer MSC-based grafts that would recapitulate the morphogenetic processes and endochondral

ossification occurring during embryonic skeletal bone development would represent an important step forward for physiological bone repair, in line with the recently defined “developmental engineering” concepts (8). In particular, the proposed route to bone formation through cartilage remodeling and vascularisation, which is also activated during successful, natural bone fracture repair, would potentially allow to overcome issues critical to the physiological functioning of engineered bone grafts, such as osteogenic performance, resistance to hypoxic conditions and efficiency of engraftment. So far, evidence of ectopic bone tissue morphogenesis via formation of hypertrophic cartilage templates have been reported for murine embryonic stem cells (ESC) (9) and chick embryonic mesenchymal cells (10), but the paradigm has thus far not been reproduced using human ESC or clinically potentially more relevant sources such as adult human MSC (9). The present study aimed at establishing and characterizing an endochondral bone tissue engineering approach, which uses bone marrow-derived, human adult MSC. By analogy to embryonic development of long bones, we hypothesized that the stage of cartilage hypertrophy reached *in vitro* by MSC would critically impact on the process of endochondral ossification following implantation into the nude mouse model. Our results demonstrate that engineered human hypertrophic cartilaginous tissue have the potential to undergo developmental changes similar to the ones during limb formation. Therefore, this study paves the way towards a “developmental engineering” approach for the regeneration of bone.

## **RESULTS**

### **In vitro maturation of engineered hypertrophic cartilage tissues**

Since endochondral bone formation is initiated by condensation and chondrogenic differentiation of mesenchymal cells, we cultured human adult MSC in a transwell, scaffold-free system to maximize cell-cell interactions (11), using a serum-free medium supplemented with TGF $\beta$ 1 as a potent inducer of chondrogenesis (12). After one week, the resulting tissues

had deposited a loose extracellular matrix, which was faintly positive for glycosaminoglycans (GAG). These specimens will be hereafter referred to as “*pre-chondrogenic*” tissues. After 2 weeks, the resulting tissues displayed clear cartilaginous features, including positive Safranin-O staining for GAG (Fig. 1a) and large cells in lacunae embedded in abundant matrix (positive for type II collagen; Fig. 1c). As only low and localized levels of type X collagen, which marks hypertrophic chondrocytes, were detected (Fig. 1e), these specimens will be hereafter referred to as “*early hypertrophic*” tissues. At this stage, type I collagen was detected throughout the tissue (Fig. 1g), with staining intensity increased in the outer rim. In this outer rim, low levels of bone sialoprotein (BSP) were also detected (Fig. 1i), but no sign of matrix mineralization was apparent (Fig. 1k).

In order to induce a more mature hypertrophic phenotype in human MSC, cells were cultured for 3 weeks in chondrogenic medium as described above and then for a further 2 weeks in medium lacking TGF $\beta$ 1, but supplemented with  $\beta$ -glycerophosphate and l-thyroxin (13, 14). This culture protocol maintained the chondrogenic features, namely GAG and type II collagen expression (Fig. 1b, 1d), but also promoted abundant and widespread accumulation of type X collagen (Fig. 1f). The outer rim of the specimens was uniformly positive for type I collagen (Fig. 1h) and developed a distinct mineralized collar (Fig. 1l), strongly positive for BSP (Fig. 1j). This histological pattern is characteristic of what was previously defined as “chondro-osseous rudiment” (15), and therefore specimens at this stage will be hereafter referred to as “*late hypertrophic*” tissues. The progression of chondrogenesis through hypertrophy and mineralization between 2 and 5 weeks of *in vitro* culture was paralleled by increased expression of type X collagen (*CX*; 4.2-fold), *MMP13* (3.7-fold), core-binding factor alpha subunit 1 (*Cbfa1*; 7.2-fold), osteocalcin (*OC*; 430-fold), and bone sialoprotein (*BSP*; 5.7-fold) transcripts (Fig. 1m, 1n). Following hypertrophic differentiation, phenotypic analysis by cell flow cytometry demonstrated an overall decrease in the expression of markers typical for undifferentiated MSC (CD73, CD90, CD105, CD146) and an increase of alkaline phosphatase

(ALP; Fig. S1). Vascular endothelial growth factor (VEGF) transcript, released protein and matrix-bound protein were detected at similar levels throughout the culture stages (Fig. S2).

### **Progression of bone development following *in vivo* implantation of hypertrophic cartilage constructs**

Both *pre-chondrogenic*, *early hypertrophic* and *late hypertrophic* constructs were implanted subcutaneously into nude mice and harvested after 4 and 8 weeks. *Pre-chondrogenic* constructs could not be recovered following implantation, as they were likely resorbed by the host environment. Following 4 weeks *in vivo*, *early hypertrophic* samples developed into structures containing cells embedded in large lacunae within an extracellular matrix rich in GAG (Fig. 2a) and type X collagen (Fig. 2e), while BSP deposition was confined in the outer rim (Fig. 2i). Eight weeks after implantation, the extracellular matrix extensively remodeled, displayed reduced GAG levels (Fig. 2b) and diffuse deposition of BSP (including the central regions, Fig. 2j). In the central region BSP overlapped with type X collagen (compare Fig. 2j to Fig. 2f). Four weeks after implantation, *late hypertrophic* samples displayed two distinct regions: an outer osteoid tissue, which resembled a bony collar, and an inner cartilaginous region, which was faintly positive for GAG (Fig. 2c). Type X collagen was present predominantly in the peri-cellular space (Fig. 2g), partially overlapping the accumulation of BSP (Fig. 2k). After 8 weeks *in vivo*, the cartilaginous template was almost completely resorbed, and bone ossicles appeared also in the central region (Fig. 2d, 2h, 2l).

Taken together, these results indicate that (i) a hypertrophic cartilaginous template is required to prime the endochondral ossification process, and (ii) the maturation of *early hypertrophic* samples toward the endochondral route progresses upon *in vivo* implantation, albeit it being delayed in comparison to implantation of *late hypertrophic* tissues.

### ***In vivo* remodeling and vascularisation of *late hypertrophic* cartilage**

To assess if the progression of tissue morphogenesis *in vivo* closely resembled normal endochondral ossification, *late hypertrophic* specimens were analyzed in more detail. Four weeks after implantation, the outer regions corresponding to the bony collar were positive for MMP-13 (Fig. 3a), which is typically expressed by late hypertrophic chondrocytes or osteoblasts and acts upstream of initiating angiogenesis (16). Indeed, capillary vessels positive for CD31 (PECAM-1) began to penetrate the outer matrix (Fig. 3b, 3c), consistent with the requirement to transport **host** osteoclasts, nutrients and pro-apoptotic signals to the internal hypertrophic cartilaginous template (1, 17). After 8 weeks *in vivo*, cartilaginous regions undergoing remodeling were surrounded by multi-nucleated cells of the osteoclastic lineage, as revealed by their positive staining for two markers typically expressed at this stage of resorption (18), namely tartrate-resistant acid phosphatase (TRAP; Fig. 3d) and MMP-9 (Fig. 3e). The ongoing, active matrix digestion process was confirmed by abundant expression of the so-called cryptic epitope of aggrecan (DIPEN; Fig. 3f), which is exposed specifically upon MMP-mediated cleavage of aggrecan (19).

#### **Activation of signalling pathways involved in normal endochondral ossification**

We next performed a real-time RT-PCR and *in situ* hybridization (ISH) analysis of the expression of key components of signalling pathways, which are known to be required for normal endochondral ossification during embryonic development (20, 21, 22). In particular, the expression of Indian Hedgehog (IHH) as upstream signal, its receptor Patched1 (PTCH1) and GLI1 as mediator of IHH signal transduction was assessed. As expected, all these genes were either not expressed or expressed at very low levels in post-expanded MSC, while their expression levels were markedly increased in the *early hypertrophic* and even more in the *late hypertrophic* constructs (IHH: 5.2 fold, PTCH1: 3.0 fold, GLI1: 7.8-fold - when comparing *late* to *early hypertrophic* tissues; Fig. 4a). In contrast, the expression of the other two Hedgehog ligands present in vertebrate species including humans (Sonic Hedgehog: SHH and



Desert hedgehog: DHH) was not activated (Fig. 4a). Similar to IHH, BMPs (BMP-2: 36.5 fold, BMP-4: 7.8 fold, BMP-7: 169.4 fold), Parathyroid hormone-related protein (PTH1LH: 30.8 fold) and its receptor (PTHR1: 6.2 fold) were significantly up-regulated in *late* as compared to *early hypertrophic* tissues (Fig. 4a). This shows that the progression towards endochondral ossification, both *in vitro* and *in vivo*, is paralleled by the activation and/or up-regulation of the key signalling pathways involved in endochondral bone formation during embryonic limb skeletal morphogenesis (Fig. 4a-4d, Fig. S3). **The human specificity of the ISH probes further allows to conclude that implanted cartilaginous templates included not only cells which provided signals initiating endochondral ossification (i.e., IHH), but also cells which responded to such signals (i.e., by expressing GLI1), and thus activated the required morphogenetic pathways (i.e., by expression of BMP-7).** The functional importance of IHH signal transduction was further evidenced by the fact that its selective inhibition by cyclopamine administration (23) to *in vitro* cultured cartilaginous templates derived from human MSC completely blocked their morphogenesis and maturation (Fig. 4e, f, g).

### **Characterization and quantification of the engineered endochondral bone tissue**

Quantitative microtomography ( $\mu$ CT) of explants confirmed that deposition of mineralized matrix in *early hypertrophic* samples was negligible at 4 weeks after implantation and remained confined to the outer rim at 8 weeks (Fig. 5a, b). In contrast, *late hypertrophic* constructs contained abundant peripheral mineral deposits already at 4 weeks and displayed an interconnected network of trabeculae throughout the core at 8 weeks after implantation (Fig. 5c, d). Not only the quantity (Fig. 5e), but also the stage of maturation of the mineralized matrix was more advanced in *late hypertrophic* tissues, as revealed by the significantly higher mineral density (Fig. 5f) at both time points and by the lamellar morphology of the osteoid (Fig. 5g, h). The complete loss of type X collagen in the lamellar structures of *late hypertrophic* tissues after 8 weeks *in vivo* contrasted with the remaining expression and partial

overlap with osteocalcin in the *early hypertrophic* constructs (Fig. 5i, j). This result indicates that shortened maturation *in vitro* may delay progression of endochondral ossification *in vivo*. To further investigate whether prolonged maturation *in vivo* would be able to compensate for shorter periods of *in vitro* culture, *early hypertrophic* constructs were analyzed 11 weeks after implantation, which results in a total period of *in vitro* and *in vivo* development equal to *late hypertrophic* samples analyzed 8 weeks after implantation. Interestingly, *early hypertrophic* samples analyzed after 11 weeks displayed features of mature bone formation, although they remained significantly smaller than *late hypertrophic* constructs after 8 weeks of implantation (Fig. S4). It is currently debated whether the bone formed by endochondral ossification is exclusively generated by osteoblastic progenitors delivered by the vasculature or also by cells within the hypertrophic cartilaginous template (15). We thus assessed our explants by ISH for the presence of human *Alu* repeat sequences. The presence of positive cells within the trabeculae of the bone and the surrounding soft tissue demonstrates an active contribution of the human MSC in the newly formed bone tissue and thus an effective intrinsic osteogenic property of the engineered grafts (Fig. 5k, l). Due to the non-clonality of the original human MSC population, our results are however not conclusive with respect to the controversial issue whether bone cells derive by direct phenotypic conversion of hypertrophic chondrocytes or by direct osteoblastic differentiation of different MSC subsets (15). Endochondral skeletogenesis is known to generate a marrow microenvironment, which is prerequisite for hematopoiesis (24). Morphological analysis provided evidence for hematopoietic foci in some areas neighboring the bone matrix generated by the human adult MSC (Fig. S5a), which further validates the endochondral ossification process. Support for possibly ongoing hematopoiesis in these foci was provided by the presence of CD146+ stromal cells (25), which were detected in the tissue constructs (Fig. S5b).

## **DISCUSSION**

In this study, we report a hitherto not described capacity of adult expanded human MSC to generate *de novo* bone tissue *in vivo* through endochondral ossification. The observed endochondral morphogenesis bears striking features of normal endochondral ossification as is typical for limb skeletal development, namely (i) cellular condensation and hypertrophic chondrogenesis, (ii) functional dependence on IHH signalling, (iii) formation of a bony collar by perichondral ossification, (iv) MMP-mediated matrix remodeling, vascularisation, and osteoclastic activity, (v) bone matrix deposition over the resorbed cartilaginous template, and (vi) formation of complete bone tissue, which likely includes functional hematopoietic foci.

Our study shows that activation of the endochondral ossification program requires a mature hypertrophic cartilaginous template obtained *in vitro* (*late hypertrophic* constructs) or *in vivo* (*early hypertrophic* constructs), in which cells expressing high levels of type X collagen are surrounded by osteoblastic cells expressing high levels of BSP. These observations are consistent with the fact that the development of long bones is triggered by the formation of a vis-à-vis pattern between hypertrophic chondrocytes at the lateral aspects of the rudiment and differentiating osteoblasts in the surrounding mesenchymal tissues (26). Interestingly, the progression of bone formation *in vivo* was regulated by the developmental stage and size of the hypertrophic cartilaginous constructs generated *in vitro* for implantation. The need for a fine coordination between the stage of hypertrophy reached *in vitro* and the time required to achieve endochondral ossification *in vivo* is further confirmed by the reported absence of ‘frank’ trabecular bone tissue in a previous study where chondrogenically differentiated human MSC were implanted ectopically (27).

The ectopic, “inert” subcutaneous implantation model used for this study allowed us to demonstrate that the hypertrophic cartilaginous constructs contained all necessary “biological instructions” to initiate a developmental process with similarities to what is observed during limb skeletal bone development (i.e. activation and up-regulation of IHH, BMP and PTHLH

signalling, and self-organization of the tissue in a spatially and temporally coordinated manner). The experimental concept described here is in line with the ideas of “developmental engineering”, in that an engineered construct is able to progress through development and differentiation into a structured tissue in a manner comparable to normal progression of embryonic development (28). In particular, no instructive external signals seem required after implantation and MSC were able to form bone tissue without a ceramic/mineral substrate, which is typically necessary to ‘prime’ differentiation into functional osteoblasts (6, 29). This may open the possibility either to use the tissue itself as a scaffold (this study) or - in case a predefined size and shape is required - to introduce different types of materials (e.g. synthetic polymers) which can be easier processed or tailored with respect to their physical and/or mechanical properties and could be better biodegradable than ceramic scaffolds (30).

By mimicking normal developmental processes during bone engineering and repair, the endochondral route of MSC differentiation into bone we describe here could provide significant biological and practical advantages in comparison to engineering approaches relying on intra-membranous ossification. For example, implantation of a hypertrophic cartilage template in contrast to a construct delivering undifferentiated MSC or osteoblasts, may be better suited to overcome the initial lack of vascularisation and associated hypoxia. In fact, hypertrophic chondrocytes can accelerate graft invasion by blood vessels (e.g. by release of angiogenic factors and production of MMPs) and are physiologically functional even at reduced oxygen tension (31). Moreover, considering the different composition and metabolism of bone tissues formed by intra-membranous and endochondral morphogenesis (32), and the concept that bone repair processes should avoid major differences with normal developmental programs (33), MSC-driven bone formation via endochondral ossification could lead to more successful engraftment. Our study warrants further investigations towards a clinical implementation of the developed paradigm, including (i) scaling-up of the constructs implanted and (ii) orthotopic implantation in an immunocompetent animal model

as biomechanical and inflammatory/immune mechanisms likely participate in regulating the bone forming potential of the hypertrophic templates. Finally, it will be interesting to assess **the contribution of host cells in the observed processes, possibly in immunocompetent models (34), and** if hypertrophic cartilage constructs without cells might be able to initiate endochondral ossification by recruiting host progenitors. Experiments in this direction would open the attractive possibility to manufacture biological off-the-shelf grafts relying on the properties of a cell-laid extracellular matrix.

In conclusion, we describe the first model based on human adult MSC, which recapitulates certain aspects of normal endochondral bone formation during embryonic development. The model system described is of clinical relevance for bone engineering and/or regeneration. Furthermore, it can be used to study the cellular/molecular mechanisms that control endochondral bone formation by human adult MSC isolated from both normal individuals and patients affected by specific diseases.

## **MATERIALS AND METHODS**

All human samples were collected with informed consent of the involved individuals and all mouse experiments were performed in accordance with Swiss law. All studies were approved by the responsible veterinary and ethics authorities. Human mesenchymal stem cells (MSC) were expanded for 2 passages and cultured in transwell ( $5 \times 10^5$  cells/insert) for 1 week or 2 weeks in a chondrogenic medium (with TGF $\beta$ 1; “*pre-chondrogenic*” and “*early hypertrophic*” respectively), or for 3 weeks in chondrogenic medium followed by 2 weeks in a hypertrophic medium (without TGF $\beta$ 1 and with beta-glycerophosphate and thyroxine; “*late hypertrophic*”). During *in vitro* culture, selected transwells were supplemented with KAAD-cyclopamine and cultured for 5 weeks. The resulting tissues were analysed histologically, immunohistochemically, biochemically (glycosaminoglycans and DNA) and by real time RT-PCR. Both *pre-chondrogenic*, *early hypertrophic* and *late hypertrophic* tissues were

implanted subcutaneously in nude mice and retrieved after 4 or 8 weeks. Tissue development *in vivo* was evaluated histologically, immunohistochemically and by  $\mu$ CT. The survival and contribution to bone formation by MSC was evaluated with *in situ* hybridization for human Alu sequences. Non-radioactive RNA *in situ* hybridization analysis on paraffin sections (*in vitro* and *in vivo* constructs) was also performed using human antisense riboprobes specific for IHH, GLI1 and BMP7. A more complete and detailed description of the methods is included in the online supplemental information.

## **ACKNOWLEDGMENTS**

We are grateful to Silvia Reginato and Dr. Andrea Banfi for the expert assistance with fluorescence techniques, to Dr. Chitragada Acharya for the invaluable help in human MSC screening, to Dr. Roberto Gianni-Barrera for the expert assistance in VEGF quantization, to PD Dr. Luigi Tornillo for the support in human bone analysis, to Prof Lee Ann Laurent Applegate and Prof. Dominique Pioletti for kindly providing human positive controls for ISH, and to Prof. Bert Mueller for the help in obtaining and interpreting  $\mu$ CT data. The work was partially funded by the Swiss National Science Foundation (grants 310030-120432 to AS and 31003A-113866 to RZ), by the European Space Agency (grant “ERISTO” to IM) and by a European Marie Curie Reintegration Grant (PERG05-GA-2009-246576 to JLR).

## **REFERENCES**

1. Kronenberg HM (2003) Developmental regulation of the growth plate. *Nature* 423:332-336.
2. Noonan KJ, Hunziker EB, Nessler J, Buckwalter JA (1998) Changes in cell, matrix compartment, and fibrillar collagen volumes between growth-plate zones. *J Orthop Res* 16:500-508.

3. Bianco P, Cancedda FD, Riminucci M, Cancedda R (1998) Bone formation via cartilage models: the "borderline" chondrocyte. *Matrix Biol* 17:185-192.
4. Meijer GJ, de Bruijn JD, Koole R, van Blitterswijk CA (2007) Cell-based bone tissue engineering. *PLoS Med* 4:e9
5. Ashton BA, et al. (1980) Formation of bone and cartilage by marrow stromal cells in diffusion chambers in vivo. *Clin Orthop Relat Res* 151:294-307.
6. Martin I, Muraglia A, Campanile G, Cancedda R, Quarto R (1997) Fibroblast growth factor-2 supports ex vivo expansion and maintenance of osteogenic precursors from human bone marrow. *Endocrinology* 138:4456-4462.
7. Quarto R, et al. (2001) Repair of large bone defects with the use of autologous bone marrow stromal cells. *N Engl J Med* 344:385-386.
8. Lenas P, Moos MJ, Luyten F (2009) Developmental Engineering: A new paradigm for the design and manufacturing of cell based products. Part I: From three-dimensional cell growth to biomimetics of *in vivo* development. *Tissue Eng Part B Rev* 15:381-394
9. Jukes JM, et al. (2008) Endochondral bone tissue engineering using embryonic stem cells. *Proc Natl Acad Sci USA* 105:6840-6845.
10. Oliveira SM et al. (2009) Engineering endochondral bone: in vivo studies. *Tissue Eng Part A* 15:635-643.
11. Murdoch AD, et al. (2007) Chondrogenic differentiation of human bone marrow stem cells in transwell cultures: generation of scaffold-free cartilage. *Stem Cells* 25:2786-2796.
12. Johnstone B, Hering TM, Caplan AI, Goldberg VM, Yoo JU (1998) In vitro chondrogenesis of bone marrow-derived mesenchymal progenitor cells. *Exp Cell Res* 238:265-272
13. Mackay AM, et al. (1998) Chondrogenic differentiation of cultured human mesenchymal stem cells from marrow. *Tissue Eng* 4:415-428.

14. Mueller MB, Tuan RS (2008) Functional characterization of hypertrophy in chondrogenesis of human mesenchymal stem cells. *Arthritis Rheum* 8:1377-1388.
15. Muraglia A, et al. (2003) Formation of a chondro-osseous rudiment in micromass cultures of human bone-marrow stromal cells. *J Cell Sci* 116:2949-2955.
16. Stickens D, et al. (2004) Altered endochondral bone development in matrix metalloproteinase 13-deficient mice. *Development* 131:5883-5895.
17. Gerber H-P, et al. (1999) VEGF couples hypertrophic cartilage remodeling, ossification and angiogenesis during endochondral bone formation. *Nat Med* 5:617-618.
18. Ortega N, Behonick D, Stickens D, Werb Z (2003) How proteases regulate bone morphogenesis. *Ann N Y Acad Sci* 995:109-116.
19. Singer II et al. (1995) VDIPEN, a metalloproteinase-generated neoepitope, is induced and immunolocalized in articular cartilage during inflammatory arthritis. *J Clin Invest* 95:2178-2186.
20. St-Jacques B, Hammerschmidt M, McMahon AP (1999) Indian hedgehog signaling regulates proliferation and differentiation of chondrocytes and is essential for bone formation. *Genes Dev.* 13:2072-86.
21. Karaplis AC, et al.(1994) Lethal skeletal dysplasia from targeted disruption of the parathyroid hormone-related peptide gene. *Genes Dev.* 8:277-89.
22. Yoon BS, et al. (2005) *Bmpr1a* and *Bmpr1b* have overlapping functions and are essential for chondrogenesis in vivo. *Proc Natl Acad Sci U S A.* 102:5062-5067.
23. Taipale J, et al. (2000) Effects of oncogenic mutations in Smoothed and Patched can be reversed by cyclopamine. *Nature* 406:1005-1009.
24. Chan CK, et al. (2009) Endochondral ossification is required for haematopoietic stem-cell niche formation. *Nature* 457:490-494.



25. Sacchetti B et al. (2007) Self-renewing osteoprogenitors in bone marrow sinusoids can organize a hematopoietic microenvironment. *Cell* 131:324-336.
26. Riminucci M, et al. (1998) Vis-à-vis cells and the priming of bone formation. *J Bone Miner Res* 13:1852-1861.
27. Pelttari K, et al. (2006) Premature induction of hypertrophy during in vitro chondrogenesis of human mesenchymal stem cells correlates with calcification and vascular invasion after ectopic transplantation in SCID mice. *Arthritis Rheum* 54: 3254-3266
28. Lenas P, Moos MJ, Luyten F (2009) Developmental Engineering: A new paradigm for the design and manufacturing of cell based products Part II. From genes to networks: tissue engineering from the viewpoint of systems biology and network science. *Tissue Eng Part B Rev* 15:395-422
29. Haynesworth SE, Goshima J, Goldberg VM, Caplan AI (1992) Characterization of cells with osteogenic potential from human marrow. *Bone*.13:81-88
30. Rezwan K, Chen QZ, Blaker JJ, Boccaccini AR (2006) Biodegradable and bioactive porous polymer/inorganic composite scaffolds for bone tissue engineering. *Biomaterials* 27:3413-3431.
31. Pfander D, Gelse K (2007) Hypoxia and osteoarthritis: how chondrocytes survive hypoxic environments. *Curr Opin Rheumatol* 9:457-462.
32. Van den Bos T, Speijer D, Bank RA, Brömme D, Everts V (2008) Differences in matrix composition between calvaria and long bone in mice suggest differences in biomechanical properties and resorption: Special emphasis on collagen. *Bone* 43:459-468.
33. Leucht P, et al. (2008) Embryonic origin and Hox status determine progenitor cell fate during adult bone regeneration. *Development* 135:2845-2854.

34. Tasso R, Fais F, Reverberi D, Tortelli F, Cancedda R (2009) The recruitment of two consecutive and different waves of host stem/progenitor cells during the development of tissue-engineered bone in a murine model. *Biomaterials* 31:2121-2129.
35. Braccini A, et al. (2005) Three-dimensional perfusion culture of human bone marrow cells and generation of osteoinductive grafts. *Stem Cells* 23:1066-1072.
36. Barbero A, Ploegert S, Heberer M, Martin I (2003) Plasticity of clonal populations of dedifferentiated adult human articular chondrocytes. *Arthritis Rheum* 48:1315-1325.
37. Dickhut A, et al. (2009) Calcification or dedifferentiation: requirement to lock mesenchymal stem cells in a desired differentiation stage. *J Cell Physiol* 219:219-226.
38. Chotteau-Lelièvre A, Dollé P, Gofflot (2006) Expression analysis of murine genes using in situ hybridization with radioactive and nonradioactively labeled RNA probes. *Methods Mol Biol* 326:61-87
39. Papadimitropoulos A, et al. (2007) Kinetics of *in vivo* bone deposition by bone marrow stromal cells within a resorbable porous calcium phosphate scaffold: an X-ray computed microtomography study. *Biotechnol Bioeng* 98:271-281.

## Figure Legends

### Figure 1. *In vitro* maturation of hypertrophic cartilage tissues engineered from human adult MSC

*In vitro* culture conditions determined the composition and structure of the tissues generated. (a, c, e, g) *Early hypertrophic* samples displayed a cartilaginous ECM rich in GAG and Col II with deposition of Col X and Col I in defined regions. (i, k) In the periphery of *early hypertrophic* samples, low BSP levels were detected but no calcium was deposited. (b, d, f, l, h, j) *Late hypertrophic* samples underwent further maturation *in vitro* and developed two distinct regions: an inner hypertrophic core (b, d, f) rich in GAG, Col II, Col X and an outer mineralized rim (b, l, h, j) with a high mineral content, Col I, and BSP. All pictures were

taken at the same magnification, scale bar = 200 $\mu$ m. The insets display low magnification overviews of the entire tissues. (m, n) Quantitative real-time RT-PCR demonstrated an up-regulation of hypertrophic (Col X and MMP-13) and osteogenic (cbfa-1, osteocalcin, BSP) markers when comparing *late* with *early hypertrophic* tissues. Post-expanded MSC remained in an undifferentiated state, but expressed both SOX-9 and Cbfa-1 in combination with high type I collagen, and low type II collagen levels. Note that all fold changes in transcript levels are shown in logarithmic scale.

**Figure 2. Development of the hypertrophic cartilage tissues following *in vivo* implantation**

The differentiation of cartilaginous constructs *in vivo* progressed according to their stage of *in vitro* maturation. (a, e, i) Four weeks after implantation, *early hypertrophic* samples had differentiated further towards hypertrophy, displaying larger lacunae, Col X accumulation and initiated BSP deposition in the outer rim. (b, f, j) Eight weeks after implantation, *early hypertrophic* samples had differentiated even further. This was evidenced by a decrease in GAG accumulation, while Col X was maintained and BSP had also been deposited within the cartilaginous core. (c, g, k) After 4 weeks, *late hypertrophic* specimens had undergone more intense remodeling, such that GAG and Col X levels were reduced, while BSP had already been deposited within the cartilaginous core. (d, h, l) After 8 weeks, the cartilaginous template was almost completely resorbed: bone structures substituted the GAG positive areas in the central region, while Col X and BSP positive areas were restricted to scattered islands. All the pictures were taken at the same magnification, scale bar = 200 $\mu$ m.

**Figure 3. *In vivo* remodeling and vascularisation of *late hypertrophic* cartilage implants**

(a) The observed remodeling resembles the temporal and spatial changes indicative of ongoing endochondral ossification. Hypertrophic chondrocytes located in the bony collar

(BC) synthesized MMP13, which is known to prepare the ECM for vascular invasion during endochondral ossification. (b, c) Newly formed vessels, identified by CD31+ endothelial cells, penetrated the outer matrix and reached the inner core in close proximity to the cartilaginous areas undergoing remodeling (arrows). (d, e) The cartilaginous regions were colonized by TRAP-positive cells synthesizing MMP9. (f) These regions were also positive for the cryptic epitope of aggrecan (DIPEN), which is produced by MMP-mediated cleavage of aggrecan. Scale bars = 100 $\mu$ m.

**Figure 4. Activation of signalling pathways involved in endochondral bone formation in embryos**

Signalling pathways typically involved in endochondral ossification were activated in the engineered samples. (a) Real-time RT-PCR analysis indicated that MSC cultured under hypertrophic conditions up-regulated the expression of genes in the IHH signalling pathway (involving IHH, GLI1 and PTCH1), BMPs and parathyroid hormone-related protein signalling (PTH1L, PTHR1). Note that all fold changes in transcript levels are shown in logarithmic scale. (b, c, d) Four weeks after implantation, the expression of representative genes was assessed by *in situ* hybridization (IHH, GLI1, and BMP7). (e-g) Functional inhibition of the IHH pathway by cyclopamine treatment significantly reduced the expression of genes involved in IHH signalling (IHH, GLI1, PTCH1), PTH signalling (PTH1L, PTHR1), as well as chondrogenic/hypertrophic genes (Col II, VEGF), and osteogenic genes (Cbfa-1, Col I, BSP). Cyclopamine also blocked the differentiation and maturation of the cartilaginous templates *in vitro*, as assessed by Safranin-O stain. Scale bars = 200 $\mu$ m (b, c, d) and 400  $\mu$ m (e, f).

**Figure 5. Morphometric analysis of the engineered bone tissue**

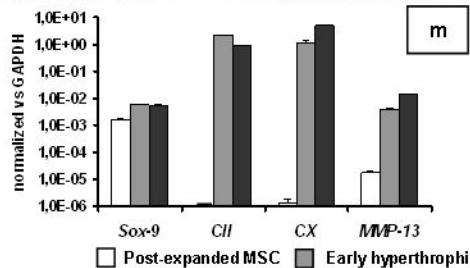
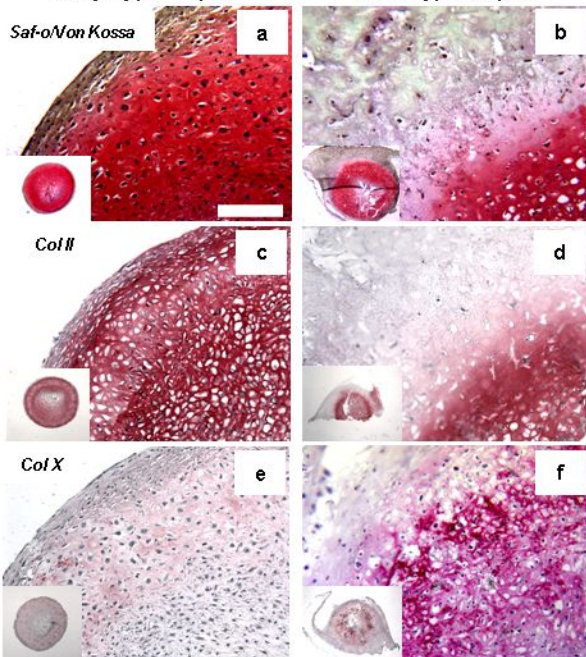
(a-d) Three-dimensional  $\mu$ CT reconstructions and (e, f) quantitative histomorphometric data (n=4) of mineral volume and density indicate higher bone quantity and more advanced

maturation of *late hypertrophic* samples (\* indicates significant differences;  $p < 0.01$ ). (g, h) Trabecular-like structures were found both in the outer bony collar and in the inner core of *late*, but not *early hypertrophic* samples (scale bar = 200 $\mu$ m). (i, j) Fluorescence characterization for Col X (red) and osteocalcin (green) demonstrated the presence of mature lamellar bone only in *late hypertrophic* samples (scale bar = 50 $\mu$ m). (k, l) *In situ* hybridization to detect human *Alu* repeat sequences and hematoxylin/eosin staining of serial sections indicate that cells derived from the human adult MSC participated in the endochondral ossification process and remained embedded within the bone matrix (scale bar = 100 $\mu$ m).

## CHONDROGENIC MARKERS

Early hypertrophic

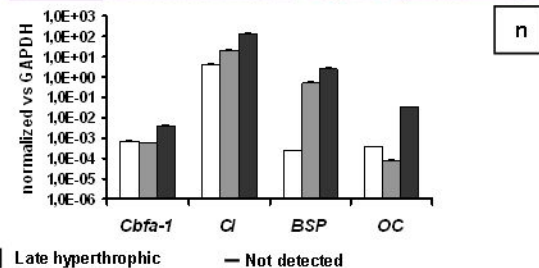
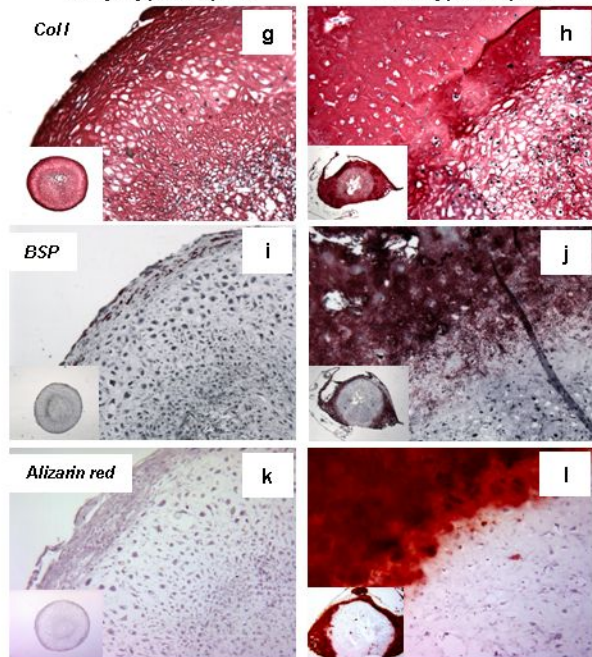
Late hypertrophic



## OSTEOGENIC MARKERS

Early hypertrophic

Late hypertrophic



## EARLY HYPERTROPHIC

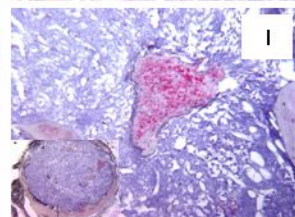
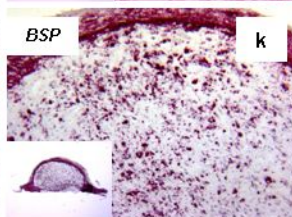
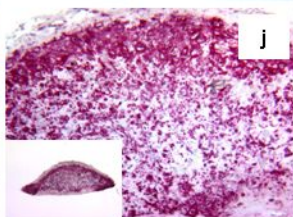
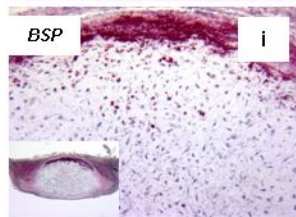
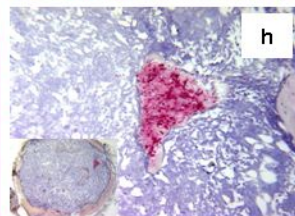
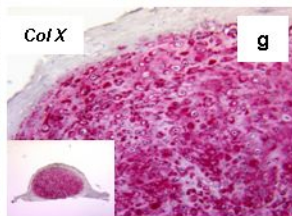
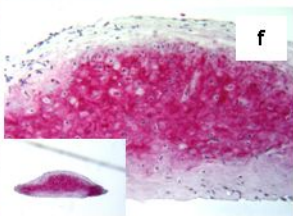
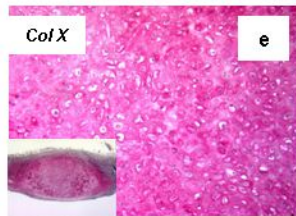
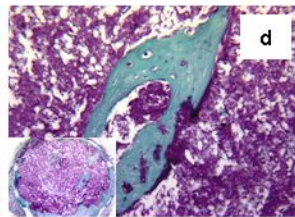
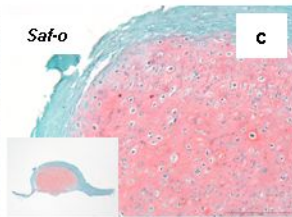
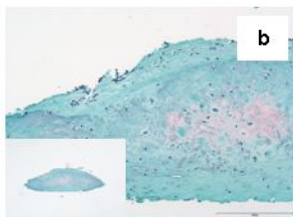
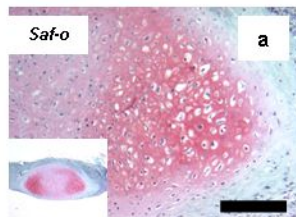
4 weeks in vivo

8 weeks in vivo

## LATE HYPERTROPHIC

4 weeks in vivo

8 weeks in vivo



*MMP13*

**a**

BC

**b**

ColX CD31

**c**

ColX CD31

**d**

*TRAP*

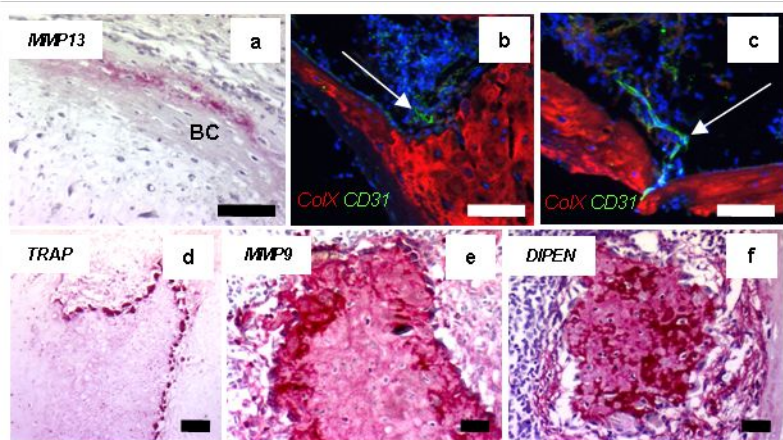
**e**

*MMP9*

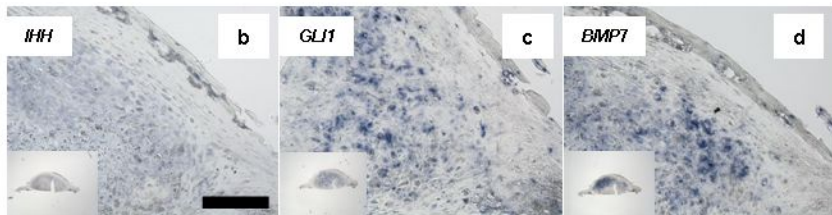
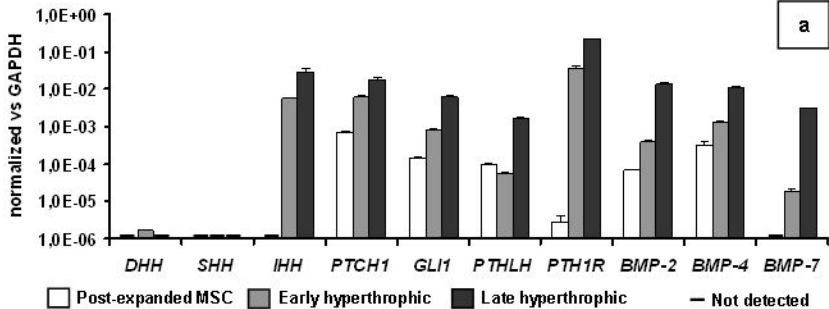
**f**

*DIPEN*

**g**

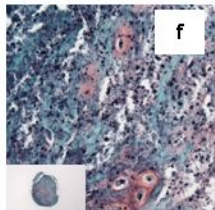
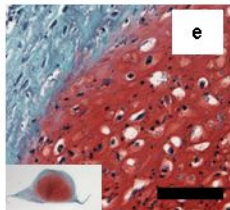






**Control**

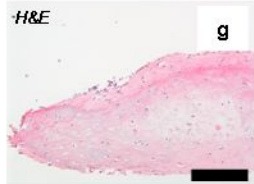
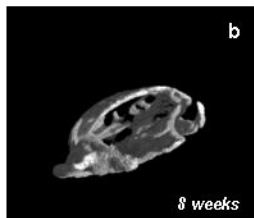
**Cyclopamine treated**



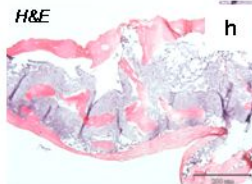
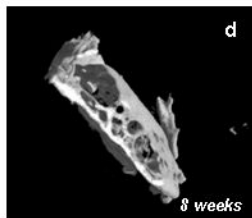
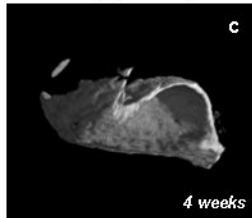
	Fold differences (Cyclopamine vs ctr)	Up (↑)/down (↓) regulation
<i>IHH</i>	10.4	↓
<i>PTCH1</i>	37.4	↓
<i>GLI1</i>	40.3	↓
<i>PTHLH</i>	3.7	↓
<i>PTH1R</i>	4.8	↓
<i>Cil</i>	8.6	↓
<i>VEGF</i>	2.8	↓
<i>MMP13</i>	6.1	↑
<i>Cbfa1</i>	2.7	↓
<i>Cl</i>	2.3	↓
<i>BSP</i>	12.1	↓

**g**

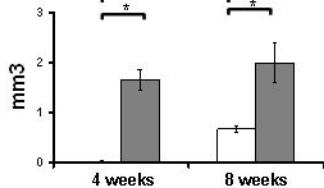
Early hypertrophic



Late hypertrophic



Mineral volume



Mineral density

